Rotational spectra, structures, and dynamics of small $Ar_m-(H_2O)_n$ clusters: The $Ar-(H_2O)_2$ trimer

E. Arunan[a)]
Department of Inorganic and Physical Chemistry, Indian Institute of Science, Bangalore, India 560 012

T. Emilsson[b)] and H. S. Gutowsky[c)]
Noyes Chemical Lab, University of Illinois, Urbana, Illinois 61801

Rotational-tunneling spectra for $Ar-(H_2O)_2$ and $Ar-(D_2O)_2$ have been observed with the Balle–Flygare Fourier transform microwave spectrometer. The tunneling levels of the trimer appear to correlate with those of the water dimer. The ''a'' dipole transitions from the A_1^+ and E^+ states of $Ar-(H_2O)_2$ and A_1^+, B_1^+, and E^+ states of $Ar-(D_2O)_2$ could be fit to a semirigid rotor Watson Hamiltonian. However, only the E^+ states give ''b'' dipole transitions near rigid rotor predictions. The ''b'' dipole transitions for A_1^+ and B_1^+ are rotational-tunneling spectra. For $Ar-(D_2O)_2$, these transitions were observed and the donor–acceptor interchange tunneling splitting is determined as 106.3 MHz, compared to about 1100 MHz in the free $(D_2O)_2$. From this splitting, the barrier for interchange tunneling is calculated to be 642 cm^{-1}. This splitting for $Ar-(H_2O)_2$ is estimated as 4–5 GHz. This and the spin statistical weight of 0 for the B_1^+ state have made it difficult to observe the ''b'' dipole rotational tunneling spectra for $Ar-(H_2O)_2$. From the rotational constants for $(H_2\,{}^{18}O)$ containing trimers, the O–O distance in the trimer is estimated as 2.945 Å. This is significantly (0.035 Å) shorter than the O–O distance reported for water dimer. The Ar is located on the ''b'' axis of the water dimer. Assuming the water to be a structureless sphere in the trimer, leads to Ar-c.m.(H_2O) distance of 3.637 Å, very close to the same value in the $Ar-H_2O$ dimer.

I. INTRODUCTION

The $Ar_m(H_2O)_n$ system has attracted much interest as a model for hydrophobic interactions. Many experimental[1–5] and theoretical[6–9] studies on its simplest species, $Ar-H_2O$ dimer, have appeared during the last decade. In a classic series of papers culminating in Ref. 10, Cohen and Saykally obtained a highly accurate and detailed intermolecular potential for this challenging dimer. The main objective in studying these weakly bound systems is to be able to model their dynamics and the bulk interactions, and hence, it is important to go beyond the dimer. With this in mind we started preliminary studies several years ago of the smaller $Ar_m-(H_2O)_n$ complexes.[11] Since then, a detailed report has been given for the Ar_2-H_2O trimer[12] and Ar_3-H_2O tetramer.[13] This paper presents our results for the $Ar-(H_2O)_2$ trimer and some of its isotopomers.

The totally protonated or deuterated forms of $Ar-H_2O$ (pseudolinear) and Ar_2-H_2O (T-shaped) exhibit two series of rotational transitions. They are assigned to internal rotor states of the H_2O/D_2O, the upper series correlated with the $O_{0,0}$ rotational state of free water and the lower series with the $1_{0,1}$ state. This similarity between the dimer and trimer is heightened by finding that the hyperfine interaction constants of the water are nearly identical in the two clusters,[5,12] as must be the dynamic states of the water and the average projection of the C_2 axis on to the inertial frame. The insensitivity of the rotational state of water to its weak interaction with one or two argons implies that in $Ar-(H_2O)_2$, The rotational states of the $(H_2O)_2$ dimer could correlate with those of the *free* dimer. This is supported in quantitative terms by MMC (molecular mechanics for clusters)[14] calculations, which give equilibrium stabilities of 1950 and 2317 cm^{-1} for $(H_2O)_2$ and $Ar-(H_2O)_2$, respectively.[15] This small increment in stability describes the Argon being stuck weakly to the side of the $(H_2O)_2$ dimer as shown in Fig. 1. This weakness leads one to expect trimer energy levels correlated with those of the dimer. We give a brief summary of the latter as an aid in the present study.

Theoretically and experimentally, the water dimer is probably the most extensively studied H-bonded complex.[16] In it, different tunneling pathways permit each of the four hydrogens to participate in the H-bonding. Two types of tunneling occur. The first type involves a simple two-fold rotation of either or both of the two water molecules about its C_2 symmetry axis, giving permutations such as (12), (34) or (12)(34) in Fig. 1. The other type, interconversion tunneling, interchanges proton donor and proton acceptor roles in the dimer by permutations such as (ab)(13)(24). Dyke has shown that the dimer, with the C_s symmetry of Fig. 1 belongs to the G_{16} molecular symmetry group.[17] The ground vibrational level is eight-fold degenerate and it splits into six levels as a

a)Author to whom correspondence should be addressed. Electronic mail: arunan@ipc.iisc.ernet.in
b)Current address: APL Engineered Materials, Urbana, IL 61801.
c)Deceased (January 13, 2000).

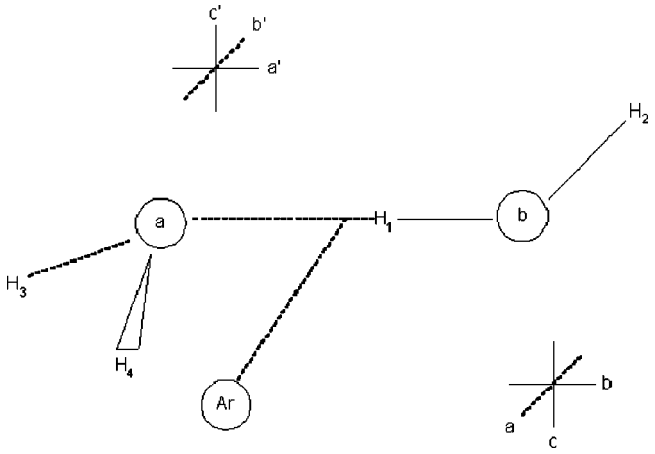

FIG. 1. Structure of $Ar-(H_2O)_2$ trimer. The "abc" axes are the principal axes for the trimer and the "a′b′c′" axes are for the $(H_2O)_2$ dimer.

result of the multidimensional tunneling. The rotational states of A' symmetry give rotational-tunneling sublevels A_1^+, B_1^+, E^+, A_2^-, B_2^-, and E^- symmetry while rotational states of A'' symmetry give sublevels of A_1^-, B_1^-, E^-, A_2^+, B_2^+, and E^+ symmetry. The overall selection rules are $A_1^+ \leftrightarrow A_1^-$, $B_1^+ \leftrightarrow B_1^-$, $A_2^+ \leftrightarrow A_2^-$, $B_2^+ \leftrightarrow B_2^-$, and $E^+ \leftrightarrow E^-$. For the fully protonated species the spin statistical weights are 1, 0, 3, 6, and 3 for A_1, B_1, A_2, B_2, and E states, and for the fully deuterated species they are 21, 15, 3, 6, and 18. To a first approximation, the levels with subscripts 1 and 2 split from each other due to tunneling of protons in the H bond acceptor, the splitting being about 200 GHz in $(H_2O)_2$ and 9 GHz for $(D_2O)_2$.[18] These levels split further into three levels each due to the donor–acceptor interchange tunneling, leading to a doubly degenerate E state close to the unperturbed level flanked by A and B states (see Fig. 2 of Ref. 16 for details). This splitting is about 20 GHz for $(H_2O)_2$ and 1 GHz for $(D_2O)_2$.[16] Only the E states of $(H_2O)_2$ give spectra of the rigid rotor type and the A and B states give rotational-tunneling spectra. With these observations at hand, we turn to the results for $Ar-(H_2O)_2$.

II. EXPERIMENT

The $Ar-(H_2O)_2$ rotational-tunneling spectra were observed with the Balle–Flygare Fourier transform microwave spectrometer described in detail elsewhere.[19] Argon was used as carrier gas with about 10% of it bubbled through H_2O kept at ambient conditions. The backing pressure was typically 0.75 atm and the nozzle diameter was 1 mm. Isotopically enriched D_2O (99.5%) and $H_2\,^{18}O$ (70%) were used for studies on the trimer isotopomers. The presence of Ar and H_2O in the species observed was ensured by changing the carrier gas to first run Ne and by bypassing the H_2O bubbler. The optimum microwave pulse required for the "b" dipole (H_2O-H_2O axis) transitions was 0.3 μs and it was $\approx$1 μs for the "a" [the Ar to c.m. of $(H_2O)_2$ axis] dipole transitions. All the Ar_m-H_2O transitions for $m=1$, 2, and 3 required about 3 μs. Hence, the optimum pulse could be used to differentiate the $Ar_m-(H_2O)_n$ clusters broadly. Initial searches with H_2O covered a broad spectral range wherein all the isotopomer transitions were eventually found. This was helpful in assigning $Ar-(H_2\,^{18}O)_2$, $Ar-(H_2\,^{18}O-H_2O)$ and $Ar-(H_2O-H_2\,^{18}O)$ isotopomers' spectra as the $H_2\,^{18}O$ sample was only 70% enriched with ^{18}O and the parent isotopomer lines could be seen during the search with $H_2\,^{18}O$.

III. RESULTS

A. Search and assignment for $Ar-(H_2O)_2$

As in FTMW work on a number of other complexes, the first lines of $Ar-(H_2O)_2$ were found while searching for other complexes, in this case $C_6H_6-H_2O$, $Ne_m-(H_2O)_n$ and $Ar_2-(H_2O)$. We observed some transitions of some complexes containing Ne and H_2O, during our work on $C_6H_6-H_2O$ dimer.[20] The presence of Ne could be easily ascertained by adding a few percent Ar, which almost always kills the signal from a Ne complex. Presumably, Ar competes with Ne and succeeds in forming the complex. Interestingly, during one such test a new much stronger line appeared at 7992.087 MHz on addition of Ar, which eventually proved to be the "b" dipole $0_{00} \rightarrow 1_{11}$ transition of the E^+ state of $Ar-(H_2O)_2$. Our initial search for Ar_2-H_2O used predictions from a structure calculated by Chalasinski *et al.*[7] On the basis of their structure, the $0_{00} \rightarrow 1_{01}$ transition for the Ar_2-H_2O was predicted to be around 4150 MHz. A search in that region, almost immediately, led to a pair of lines at 4167.2019 and 4167.4805 MHz. These two lines are the $0_{00} \rightarrow 1_{01}$, "a" dipole transitions of $Ar-(H_2O)_2$ from two states that correlate to A_1^+ and E^+ states of the water dimer. Our initial assumption that these lines were from Ar_2-H_2O resulted in laborious searches between 3500–4800 MHz, which turned out to be extremely beneficial in assigning several of the $Ar_m-(H_2O)_n$ complexes.[11] In this search we found two strong lines, one at 4513.4475 MHz requiring an optimum 0.3 μs pulse and the other just below at 4512.5010 MHz requiring an optimum pulse of 3.0 μs. The former line is the $1_{01} \rightarrow 1_{10}$ transition for the E^+ state of $Ar-(H_2O)_2$ and the latter is the $0_{00} \rightarrow 1_{01}$ transition of Ar_2-H_2O $\Sigma(1_{01})$ state.[12]

The three transitions of $Ar-(H_2O)_2$ listed above are $A+C$, $B+C$, and $A-C$, respectively, in terms of the rotational constants neglecting centrifugal distortion. Predicting the other transitions was straightforward and soon a total of 43 transitions, 18 "a" dipole and 25 "b" dipole, were listed. All the "a" dipole lines were doublets with one stronger than the other, but the "b" dipole lines did not show any systematic doubling. The weaker components of "a" dipole transitions were either at a higher or lower frequency than the stronger ones. The stronger transitions along with the "b" dipole ones could be fit to a semirigid rotor Watson Hamiltonian within experimental uncertainties. These lines showed some hyperfine structure, especially in the lower J transitions. The list of observed transitions with residues from the fit is given in Table I. The weaker lines of the "a" dipole transitions could be fit independently, but with much larger residues (rms deviation of 456 kHz).

In order to assign the two sets of transitions, we take a closer look at the rotational tunneling levels of the "free" water dimer. These levels can also be understood in terms of

TABLE I. Observed transition frequencies for $Ar-(H_2O)_2$ tunneling states that correlate with E^+ and A_1^+ states of the water dimer.

J'	K_p'	K_o'	J''	K_p''	K_o''	Frequency	Res.	Frequency[a]
2	1	1	2	1	2	2066.1399	−4.6	-
3	1	2	3	1	3	4124.6347	−2.7	4124.5842
1	0	1	0	0	0	4167.4805	0.6	4167.2019
2	1	2	1	1	1	7645.0615	0.1	7645.3358
2	0	2	1	0	1	8249.5475	0.5	8248.9762
2	1	1	1	1	0	9022.3684	−1.0	9022.5224
3	1	3	2	1	2	11 416.6253	−0.5	11 417.2244
3	0	3	2	0	2	12 169.1247	0.9	12 168.2219
3	2	2	2	2	1	12 496.2498	−3.3	12 496.0198
3	2	1	2	2	0	12 827.0004	−3.5	12 826.3428
3	1	2	2	1	1	13 475.1204	1.6	13 475.2230
4	1	4	3	1	3	15 135.7537	−1.4	15 136.2892
4	0	4	3	0	3	15 884.1367	−0.9	15 882.8263
4	2	3	3	2	2	16 593.3757	−0.4	16 593.4376
4	3	2	3	3	1	16 803.3249	−0.7	16 803.8224
4	3	1	3	3	0	16 842.2509	2.3	16 843.0830
4	2	2	3	2	1	17 372.3278	0.1	17 371.2739
4	1	3	3	1	2	17 848.5283	1.0	17 848.2774
2	0	2	1	1	1	4424.9426	5.9	⋯
1	1	0	1	0	1	4513.4475	0.7	⋯
2	1	1	2	0	2	5286.2665	−2.8	⋯
3	1	2	3	0	3	6592.2621	−2.2	⋯
1	1	1	0	0	0	7992.0870	−3.2	⋯
4	1	3	4	0	4	8556.6560	2.0	⋯
3	0	3	2	1	2	8948.9970	−2.0	⋯
5	2	3	5	1	4	10 368.2088	3.5	⋯
4	2	2	4	1	3	10 434.1094	3.0	⋯
6	2	4	6	1	5	10 903.9950	−3.2	⋯
3	2	1	3	1	2	10 910.3041	−1.9	⋯
5	1	4	5	0	5	11 239.4573	8.5	⋯
2	1	2	1	0	1	11 469.6750	3.3	⋯
2	2	0	2	1	1	11 558.4226	1.7	⋯
5	1	4	4	2	3	12 861.8585	3.4	⋯
4	0	4	3	1	3	13 416.5099	−0.9	⋯
2	2	1	2	1	2	13 539.7957	1.8	⋯
6	1	5	6	0	6	14 574.5571	−5.1	⋯
3	2	2	3	1	3	14 619.4198	−1.3	⋯
3	1	3	2	0	2	14 636.7523	1.7	⋯
4	2	3	4	1	4	16 077.0396	−2.6	⋯
4	1	4	3	0	3	17 603.3812	−0.7	⋯
5	0	5	4	1	4	17 699.4466	−1.9	⋯
5	2	4	5	1	5	17 912.2243	2.2	⋯
6	3	3	6	2	4	17 985.5050	0.1	⋯

[a]The rms deviation for A_1 transition is 456 kHz which is 2 orders of magnitude larger than the experimental uncertainty. They are affected by some tunneling motion, which is not considered in this work.

the four different combinations of ortho ($I=1,1_{01}$) and para ($I=0,0_{00}$) H_2O.[16] The A_1 and B_1 states have para water as both H-bond acceptor and donor. The A_2 and B_2 states have ortho water as both acceptor and donor. The E_1 state arises from para acceptor and ortho donor and the E_2 state has the opposite combination. As pointed out in the Introduction A_1, B_1, and E_1 states have comparable energy and the A_2, B_2, and E_2 states are at a much higher energy (about 5 cm^{-1}). Is it likely that the rigid rotor spectra observed from the $A_1/B_1/E_1$ states overlap with the $A_2/B_2/E_2$ states? The spin statistics of these states and the expected hyperfine splittings from the ortho ($I=1$) water provide clear evidence to suggest that such overlap does not happen. For $Ar-(H_2O)_2$, the two states observed should be A_1 and E_1, as the B_1 state has a zero-spin statistical weight. If the B_1 and B_2 states had spectral overlap, ''a'' dipole transitions would have shown a three-line pattern. Moreover, the weaker ''a'' dipole transitions did not show any evidence for hyperfine splitting which is possible for the A_2 state. The lines from the E_1 state clearly showed small hyperfine splitting (10–15 kHz for the lower J transitions) as expected for the ortho ($I=1$) H_2O. The hyperfine splitting, though clearly visible, was difficult for analysis and the center of the transition was used in the fitting. Either the $A_2/B_2/E_2$ levels are not populated in the expansion or they have not been identified yet.

For the dimer, the A_1^+ state does not show rigid rotorlike spectrum because the donor–acceptor interchange tunneling reverses the dipole moment leading to rotational tunneling spectra. However, for the trimer the interchange tunneling does not reverse the sign of ''a'' dipole, and hence, the ''a'' dipole transitions appear near rigid rotor predictions. The

TABLE II. Observed transition frequencies and splittings (MHz) for Ar–$(D_2O)_2$.[a]

J''	K_p''	K_o''	J'	K_p'	K_o'	Lower	Middle	Upper	$\Delta 1$[b]	$\Delta 2$[c]
						"a" dipole	Transitions			
0	0	0	1	0	1	3894.858	3894.890	3894.921	0.032	0.031
1	1	1	2	1	2	⋯	7122.0138	⋯	⋯	⋯
1	0	1	2	0	2	7696.4903	7696.5410	7696.5935	0.051	0.052
1	1	0	2	1	1	8455.2972	8455.3955	8455.4795	0.098	0.085
2	1	2	3	1	3	10 627.8454	10 627.8837	10 627.9292	0.038	0.045
2	0	2	3	0	3	11 323.1049	11 323.1647	11 323.2298	0.060	0.065
2	2	1	3	2	2	11 679.1923	11 679.2806	11 679.3733	0.088	0.093
2	2	0	3	2	1	12 038.4845	12 038.5829	12 038.7286	0.097	0.145
2	1	1	3	1	2	12 618.89969	12 619.0163	12 619.1580	0.119	0.142
3	1	3	4	1	4	14 078.2516	14 078.2935	14 078.3483	0.042	0.055
3	0	3	4	0	4	⋯	14 738.9941	⋯	⋯	⋯
3	2	2	4	2	3	15 498.0687	15 498.1750	15 498.3005	0.107	0.125
3	3	1	4	3	2	15 727.0330	15 727.1466	15 727.3032	0.113	0.157
3	3	0	4	3	1	15 775.1143	15 775.2397	15 775.3985	0.125	0.158
3	2	1	4	2	2	16 332.5382	16 332.7092	16 332.9029	0.171	0.193
3	1	2	4	1	3	16 694.2167	16 994.3706	16 694.5421	0.154	0.172
4	1	4	5	1	5	17 470.1181	17 470.1580	17 470.2233	0.040	0.065
4	0	4	5	0	5	⋯	17 986.3350	⋯	⋯	⋯
						"b" dipole	Transitions			
0	0	0	1	1	1	7024.926	7131.264	7237.618	106.338	106.354
1	0	1	1	1	0	3796.961	3903.225	4009.520	106.264	106.295
1	1	1	2	0	2	4353.931	4460.154	4566.425	106.266	106.271
1	0	1	2	1	2	10 252.093	10 358.375	10 464.683	106.282	106.308
2	0	2	2	1	1	4555.931	4662.066	4768.236	106.135	106.170
2	1	1	2	2	0	9695.681	9801.764	9907.891	106.083	106.127
2	1	2	2	2	1	11 603.131	11 709.315	11 815.523	106.184	106.208
2	1	2	3	0	3	8555.150	8661.323	8767.497	106.173	106.174
3	0	3	3	1	2	⋯	5957.920	6063.903	⋯	105.983
3	1	2	3	2	1	9115.506	9221.349	9327.209	105.843	105.860
3	1	3	4	0	4	⋯	12 772.431	⋯	⋯	⋯
4	0	4	4	1	3	7807.592	7913.301	8019.078	105.709	105.777
4	1	3	4	2	2	8754.194	8859.690	8965.207	105.496	105.517
5	1	4	5	2	3	8847.764	8952.881	9057.929	105.117	105.048
6	1	5	6	2	4	⋯	9680.583	⋯	⋯	⋯
5	1	4	5	0	5	⋯	10 561.294	⋯	⋯	⋯
4	2	3	5	1	4	⋯	13 061.198	⋯	⋯	⋯
4	1	4	4	2	3	⋯	14 180.587	⋯	⋯	⋯

[a]The middle lines belong to the trimer state correlating to E^+ state of $(D_2O)_2$. The lower and upper lines have contribution from A_1^+ and B_1^+ depending on K_p'' (see text).
[b]Spacing between the lower and middle frequencies.
[c]Spacing between the upper and middle frequencies. For "b" dipole transitions, the splitting is related to the donor–acceptor interchange tunneling. For "a" dipole transitions, the splitting is due to tunneling motions not considered here.

"b" dipole does reverse the sign on interchange tunneling and so the "b" dipole transitions for the A_1^+ state must have shifted by the tunneling frequency from the E^+ transitions. The tunneling frequency of 20 GHz in the dimer could be smaller in the trimer, but so far we have not been able to assign "b" dipole A_1^+ transitions. Unlike the free water dimer for which, the "a" dipole A_1^+ transitions were always at higher frequencies compared to the E^+ transitions, for the trimer the "a" dipole transitions were either at higher or lower frequencies than the E^+ transitions. This could be the case for "b" dipole transitions for the trimer as well, with much larger splitting (several GHz), making the identification of these lines more difficult. The dimer "a" axis is the "b" axis for the trimer (see Fig. 1). A detailed look at the energy levels of the trimer explains this feature in the rotational spectrum (*vide infra*).

B. Search and assignment of Ar–$(D_2O)_2$

For the fully deuterated water dimer, the spin statistical weights are 21, 15, and 18 for A_1^+, B_1^+ and E^+ states. Hence, "a" dipole transitions for all three states from the deuterated trimers could be observed. Moreover, the interchange tunneling in the *free* $(D_2O)_2$ dimer is only about 1 GHz, and so the chances of observing the "b" dipole transitions for Ar–$(D_2O)_2$ for all the three states is better compared to Ar–$(H_2O)_2$. With the approximate structure determined from the Ar–$(H_2O)_2$ rotational constants, predictions

TABLE III. Rotational (MHz) and centrifugal distortion constants (kHz), the donor–acceptor interchange tunneling frequency (MHz) and the rms deviations (kHz) for $Ar–(D_2O)_2$.

Constant	Lower[a]	Middle (E^+)[b]	Upper[a]
A	5517.41(2)	5517.465(3)	5517.36(2)
B	2280.963(4)	2280.931(1)	2280.912(5)
C	1614.014(1)	1614.0259(8)	1614.035(7)
d_1	−7.1(2)	−6.75(1)	−6.6(2)
d_2	−2.6(1)	−2.361(6)	−2.3(1)
d_j	17.5(2)	17.88(2)	18.3(3)
d_{jk}	161(1)	162.24(6)	163(1)
d_k	−157(3)	−139.9(6)	−165(3)
ν	−106.30(2)	⋯	106.42(2)
#[c]	12	35	12
rms	4.2	5.9	4.9

[a]The lower and upper transitions have contributions from A_1^+ and B_1^+ states. The table shows the results of fitting the ''b'' dipole tunneling spectra only. The corresponding ''a'' dipole transitions could be fit independently to give slightly better results in the sense that for 15 transitions, the rms deviation is only 2.3 kHz. The constants obtained are marginally different from those given here.

[b]The inertial defect for E^+ is −0.0462.

[c]Number of transitions included in the fit.

were made for $Ar–(D_2O)_2$. Soon ''a'' dipole $0_{00}\rightarrow 1_{01}$ transitions for the three states were observed at 3894.858, 3894.890, and 3894.921 MHz. All the ''a'' dipole transitions were observed as triplets with the spacing ranging from 30–200 kHz. The low J transitions were complicated by the D quadrupole splitting as well, obscuring the three-line pattern. For the high J transitions, however, the three lines were well resolved and clearly identified as arising from A_1, E_1, and B_1 states. The three progressions could be fitted independently, with an rms deviation of a few kHz. The ''b'' dipole transitions for the E^+ state were then predicted and observed readily. The 17 ''a'' dipole and 18 ''b'' dipole transitions of the E^+ state could be simultaneously fit to within experimental accuracy. Table II lists all the transitions assigned for $Ar–(D_2O)_2$.

A search for ''b'' dipole rotational-tunneling spectra for the A_1^+/B_1^+ states was planned. Initial searches with D_2O had shown a strong line about 106 MHz below the E^+ $0_{00}\rightarrow 1_{01}$ transition at 7131.264 MHz. A search 106 MHz above the E^+ transition resulted positively, suggesting that the tunneling splitting between E_1 and A_1/B_1 states is about 106 MHz. Several ''b'' dipole transitions from the A_1^+/B_1^+ states were observed as predicted. Most of these lines showed hyperfine structure due to D nuclei, but it was not well resolved for a detailed analysis. The tunneling splitting showed a notable decrease with J. Table II includes the spacing between the triplet structure for all the transitions observed. It decreases from 106.34 MHz for the $0_{00}\rightarrow 1_{11}$ transition to 105.05 MHz for the $5_{14}\rightarrow 5_{23}$ transition. Transitions from all three states could be fit independently to obtain rotational and centrifugal distortion constants as well as the tunneling frequency, assumed constant. The results are given in Table III.

C. Search and assignment of ($H_2\,^{18}O$) containing trimers

Approximate structural analysis from the rotational constants of $Ar–(H_2O)_2$ revealed that the O–O distance needed to fit the data depended on whether Ar is kept in the ''c'' axis (above or below) or in the ''b'' axis of the dimer. (See Fig. 1 for the structure and next section for details.) In order to clarify this ambiguity, predictions were made for $Ar–(H_2\,^{18}O)_2$ trimer and the two trimers with $H_2\,^{18}O$, either as H bond acceptor or donor. The predictions were different for the three cases mentioned previously. The predictions with Ar in the ''b'' axis of the dimer gave good agreement with the experimental results for the three isotopomers. Table IV lists the transitions observed for the three trimers. Table V lists the rotational and centrifugal distortion constants for the three trimers and the parent isotopomer along with rms deviations from the fit.

For the trimer with two $H_2\,^{18}O$, the results were very similar to that of the parent isotopomer. Two lines were observed for the ''a'' dipole transitions and one line was observed for ''b'' dipole transitions. The donor–acceptor interchange tunneling leads to different isotopomers for the mixed trimers ($^{18}O–^{16}O$). Hence, only one state was expected for both ''a'' and ''b'' dipole transitions. It was indeed true for the $Ar–(H_2O–H_2\,^{18}O)$ trimer (^{18}O in the donor). However, for the other trimer, $Ar–(H_2\,^{18}O–H_2O)$, *both* ''a'' and ''b'' dipole transitions showed doublets, with the spacing of a few 100 kHz. Table VI lists these lines which could be fitted independently, but the rms deviation of the 25 observed lines, 58.8 kHz, was much larger. The other three isotopomers listed in Table V did not show any evidence for such splitting. For HDO–DOH and HDO–HOD water dimer isotopomers, Karyakin *et al.*[21] observed different tunneling splitting due to the difference in reduced mass for the tunneling motion between the two. However, for all the fully protonated trimers under consideration, the change in reduced mass will be negligible as the tunneling motion involves only the hydrogen atoms in all cases. The fact that transitions from one more state have been observed for $Ar–(H_2\,^{18}O–H_2\,^{16}O)$ and not for $Ar–(H_2\,^{16}O–H_2\,^{18}O)$, strongly points to vibrational–rotational interactions such as Coriolis resonance in the former. In fact, Hu and Dyke[22] have reported Coriolis resonances in the water dimer parent isotopomer, $(H_2O)_2$. A detailed analysis of this aspect is beyond the scope of the present investigation.

IV. DISCUSSION

A. Structure of the $Ar–(H_2O)_2$

The gross features of the rotational-tunneling spectra observed for the $Ar–(H_2O)_2$ follow that of the free water dimer. The tunneling states observed could be correlated to the water dimer energy levels. We use the rotational constants of the E^+ state, which is expected to be the least perturbed by the various tunneling motions, to determine structural parameters for the trimer. It is noted that the A rotational constant (6253.031 MHz) for the trimer is closer to the $(B+C)/2$ for the water dimer (6160.7 MHz).[23] This suggests that the trimer is T-shaped with the Ar approaching the

TABLE IV. Observed transitions (MHz) for $H_2\,{}^{18}O$ containing trimers.[a]

J'	K'_{p0}	K'_o	J''	K''_p	K''_o	16–18	18–16	18–18	18–18[b]
						"a" dipole			
1	0	1	0	0	0	4049.2931	4037.8403	3933.9200	3933.7230
2	1	2	1	1	1	7413.9885	7398.6695	7189.7718	7189.6366
2	0	2	1	0	1	8009.0652	7989.0640	7774.6187	7774.2105
2	1	1	1	1	0	8780.8599	8750.3664	8543.7098	8543.4542
3	1	3	2	1	2	11 067.7737	11 046.4713	10 729.4835	10 729.6928
3	0	3	2	0	2	11 799.4941	11 776.0495	11 439.9785	11 439.2918
3	2	2	2	2	1	12 142.1408	12 107.7187	11 796.3072	11 797.1424
3	2	1	2	2	0	⋯	12 442.8400	12 155.8171	12 155.5324
3	1	2	2	1	1	13 109.9111	13 066.2893	12 751.5716	12 750.8145
4	1	4	3	1	3	14 667.3457	14 641.5605	14 213.5022	14 214.3308
4	0	4	3	0	3	15 380.7470	15 358.5792	14 892.8558	14 891.7605
4	2	3	3	2	2	16 118.0738	16 074.5483	⋯	⋯
4	2	2	3	2	1	16 927.8260	⋯	⋯	⋯
						"b" dipole			
1	1	0	1	0	1	4255.1526	4293.6455	4020.839	⋯
2	0	2	1	1	1	4437.5273	4371.4340	4430.913	⋯
2	1	1	2	0	2	5026.9466	⋯	4789.928	⋯
3	1	2	3	0	3	6337.3621	⋯	6101.521	⋯
1	1	1	0	0	0	7620.8250	7655.4646	7277.623	⋯
4	1	3	4	0	4	8311.6899	8288.0066	8080.068	⋯
3	0	3	2	1	2	8823.0270	8748.8127	8681.120	⋯
5	2	3	5	1	4	9761.0067	9853.2816	9221.013	⋯
4	2	2	4	1	3	9754.2768	9874.8704	9147.305	⋯
3	2	1	3	1	2	10 181.5150	10 315.2804	9527.906	⋯
6	2	4	6	1	5	10 389.2302	10 437.0501	9932.387	⋯
2	2	0	2	1	1	10 803.3760	10 938.7286	10 123.658	⋯
2	1	2	1	0	1	10 985.5280	11 016.3020	10 533.479	⋯
5	1	4	5	0	5	10 998.8837	10 936.2151	⋯	⋯
2	2	1	2	1	2	12 764.9623	12 880.4112	12 062.075	⋯
4	0	4	3	1	3	13 136.0065	13 060.9209	12 844.494	⋯
3	2	2	3	1	3	13 839.3294	13 941.6574	13 128.898	⋯
3	1	3	2	0	2	14 044.2361	14 073.7080	13 488.343	⋯
4	2	3	4	1	4	15 290.0557	⋯	⋯	⋯
4	1	4	3	0	3	16 912.0874	16 939.2196	⋯	⋯

[a]The column title refers to the masses of oxygen atoms in the H bond acceptor–donor for $Ar–(H_2O–H_2O)$. Table VI lists the second line observed for the 18–16 trimer in both "a" and "b" dipole transitions. The 16–18 trimer did not show any other systematic transitions within a few MHz of the E^+ level transitions.

[b]For the symmetrical 18–18 trimer A_1^+ level also gives "a" dipole semirigid rotor transitions like the parent isotopomer. The "b" dipole transitions for the A_1^+ are shifted by large tunneling splitting and have not been detected.

water dimer through the "b" or "c" axis of the dimer. However, it is about 93 MHz larger indicating some structural/dynamical changes between the dimer and trimer. The reference structure for the trimer is shown in Fig. 1.

The rotational constants reported in Tables III and V for the various isotopomers suggest a simple-minded approachto structural evaluation. The inertial defect for the $Ar–(H_2O–H_2O)$, $Ar–(H_2\,{}^{18}O–H_2O)$, $Ar–(H_2O–H_2\,{}^{18}O)$, $Ar–(H_2\,{}^{18}O–H_2\,{}^{18}O)$, and $Ar–(D_2O)_2$ are 1.6178, 1.6542, 1.6525, 1.7000, and -0.0462 a.m.u. Å^2, respectively. Even for the fully protonated isotopomers, the inertial defect of 1.65 is less than half that of the $Ar_2–H_2O$ trimer.[12] Hence, we treat the trimer as a simple triangle with two water spheres and an Argon. In this case, the following inertial equations can be used to calculate the c.m. to c.m. distance between the two water units, r, and the distance between Ar to the c.m. of the water dimer, R.

$$I_a = \tfrac{1}{2} m r^2 \tag{1}$$

$$I_b = \mu R^2, \tag{2}$$

where m is the mass of the water and μ is the reduced mass of the system. Of course, I_c would have to be the sum of these two if inertial defect were zero. Needless to say, such an analysis can give only approximate values for these distances. The rotational constants for the parent isotopomer give $r = 2.996$ Å and $R = 3.315$ Å. From these values, the Ar-c.m.(H_2O) distance can be calculated to be 3.637 Å, very close to the value reported for the global minimum of $Ar–H_2O$ dimer, 3.636 Å.[10] The $Ar–(H_2\,{}^{18}O)_2$ data give r and R values of 2.990 and 3.311 Å, respectively. The rotational constants of $Ar–(D_2O)_2$, which has an inertial defect very near 0, give 3.025 and 3.328 Å.

TABLE V. Rotational (MHz), centrifugal distortion constants and rms deviations (kHz) for the E_1^+ state of H_2O and $H_2\,{}^{18}O$ containing trimers.[a]

Constant	16–16	18–16[b]	16–18	18–18
A	6253.031(2)	5974.807(3)	5938.234(2)	5649.460(2)
B	2428.2309(4)	2356.997(1)	2366.5266(8)	2305.5919(7)
C	1739.3335(2)	1680.9227(9)	1682.8493(7)	1628.4011(5)
Δ[c]	1.6178	1.6542	1.6525	1.6997
d_1	−7.606(3)	−7.06(1)	−7.53(1)	−6.96(1)
d_2	−2.775(2)	−2.705(5)	−2.745(4)	−2.717(5)
d_j	21.170(8)	19.28(3)	20.38(2)	18.32(2)
d_{jk}	183.74(8)	175.8(1)	168.85(9)	164.59(8)
d_k	−147.2(2)	−141.2(6)	−137.1(5)	−136.6(3)
h_{jk}	−0.060(3)	⋯	⋯	⋯
h_{kj}	0.159(9)	⋯	⋯	⋯
#	43	29	32	28
rms[d]	2.7	4.9	4.6	2.9

[a]The column titles for the trimers refer to the mass of oxygen atoms in H bond acceptor-donor water molecules in $Ar-(H_2O-H_2O)$.

[b]The 18–16 trimer spectrum showed one more transition within a few hundred kHz from the "E_1^+" state transitions, see Table VI. These transitions could be fit independently, but the rms deviation was 58.8 kHz. The constants obtained were marginally different from the results for E_1^+ state reported in this table.

[c]Inertial defect in a.m.u. Å^2. For $Ar-(D_2O)_2$, the inertial defect is $\underline{-0.0462}$.

[d]The "a" dipole transitions from the A_1^+ state for both 16–16 and 18–18 trimers could be independently fit and the rms deviation is much larger at 456 kHz.

The rotational constants for the parent isotopomer and the two isotopomers with both H_2O and $H_2\,{}^{18}O$, can give a substitution O–O distance in the parent. The procedure developed by Kraitchman is described in detail by Gordy and Cook.[24] For the present case of asymmetric tops, it is convenient to use the planar moments of inertia, P, rather than I. They are defined as $P_x=\frac{1}{2}(-I_x+I_y+I_z)$ and P_y and P_z are obtained by cyclic permutation of the subscripts x, y, and z. The coordinates of the substituted atom are defined as follows:

$$|x|=\left[\frac{\Delta P_x}{\mu}\left(1+\frac{\Delta P_y}{I_x-I_y}\right)\left(1+\frac{\Delta P_z}{I_x-I_z}\right)\right]^{1/2} \tag{3}$$

TABLE VI. The second line observed for $Ar-(H_2\,{}^{18}O-H_2O)$ in all transitions (MHz) with residues (kHz) from the fit.

j'	K_p'	K_o'	J''	K_p''	K_o''	Frequency	Res.
2	1	2	1	1	1	7398.6200	−8.6
2	0	2	1	0	1	7989.1060	−15.9
2	1	1	1	1	0	8750.5497	−35.0
3	1	3	2	1	2	11 046.3814	−28.9
3	0	3	2	0	2	11 776.0391	15.4
3	2	1	2	2	0	12 443.0130	33.2
3	1	2	2	1	1	13 066.5387	88.2
4	1	4	3	1	3	14 641.4139	−95.6
4	0	4	3	0	3	15 358.4680	7.6
4	2	3	3	2	2	16 074.6336	146
2	0	2	1	1	1	4371.5520	−57.6
1	1	0	1	0	1	4293.6880	−3.1
3	0	3	2	1	2	8748.9692	−35.4
5	2	3	5	1	4	9853.1154	−75
4	2	2	4	1	3	9874.5963	−87.1
6	2	4	6	1	5	10 436.8498	63.5
3	2	1	3	1	2	10 315.0001	−0.6
5	1	4	5	0	5	10 936.2510	−82.0
2	1	2	1	0	1	11 016.1758	34.8
2	2	0	2	1	1	10 938.5238	52.3
4	0	4	3	1	3	13 061.0578	3.1
2	2	1	2	1	2	12 880.5325	−8.8
3	2	2	3	1	3	13 941.9471	54.9
3	1	3	2	0	2	14 073.451	21.6
4	1	4	3	0	3	16 938.8245	−90.7

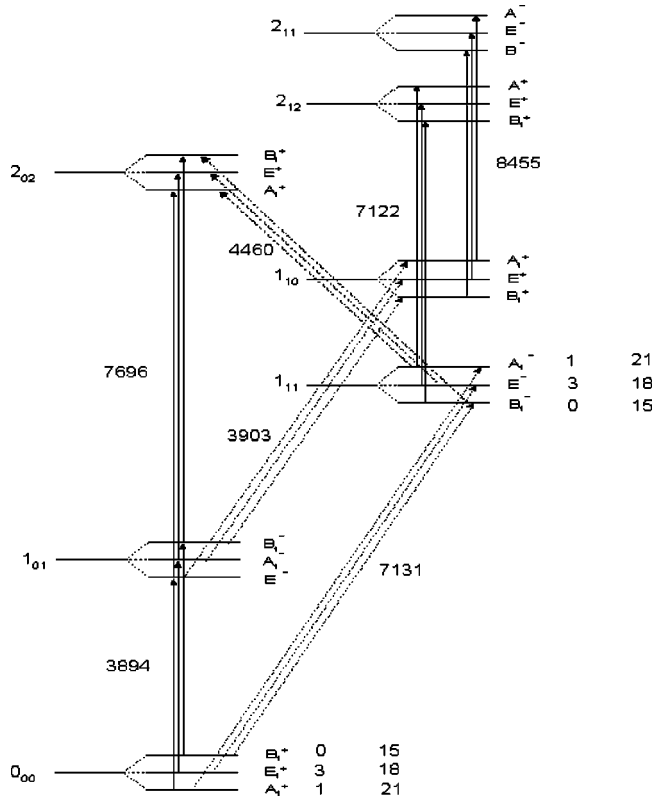

FIG. 2. Energy level diagram for the Ar–$(H_2O)_2$ trimer. The splitting between A and B levels are due to the donor–acceptor interchange tunneling. The statistical weight of the energy levels for Ar–$(H_2O)_2$ and Ar–$(D_2O)_2$ are shown next to the 0_{00} and 1_{11} levels (lowest levels in the $K=0$ and 1 manifolds). The approximate frequencies for the $E^+ \rightarrow E^-$ transition are shown. The splitting between the A and B levels is about 106 MHz for Ar–$(D_2O)_2$.

$$|y| = \left[\frac{\Delta P_y}{\mu} \left(1 + \frac{\Delta P_z}{I_y - I_z} \right) \left(1 + \frac{\Delta P_x}{I_y - I_x} \right) \right]^{1/2}. \tag{4}$$

The z coordinate is described by a similar equation in terms of ΔP_z. However, as the trimer is very nearly planar, z will be very small and the result not very reliable. Here the ΔP's give the change in P on isotopic substitution, the $I_i - I_j$ quantities refer to the moments of inertia of the parent and μ is the reduced mass for isotopic substitution $M\Delta M/(M + \Delta M)$. From these equations, x and y coordinates for the two oxygen atoms in the trimer were calculated. (The "x" axis is the "a" inertial axis and the "y" axis is the "b" inertial axis.) These were (1.772, 1.426) and (1.642, 1.516) for the two oxygen atoms. From these values the distance between the two oxygen atoms, R_{O-O}, is determined to be 2.945 Å. This is about 0.035 Å shorter than the 2.98 Å calculated for the water dimer, using isotopic substitution data with $(H_2O)_2$, $(H_2\,{}^{18}O)_2$, and $(D_2O)_2$.[23] The D substitution can lead to significant changes in the zero-point motion and the O–O distance for the dimer may be less accurate. However, the difference in rotational constants (especially A) determined for the two $^{16}O-{}^{18}O$ mixed trimers support the shorter O–O distance for the trimer compared to that of the dimer. [For the $(H_2O)_2$, studies on the mixed ^{18}O isotopomers would be useful but have not been reported to the best of our knowledge.]

As pointed out earlier, a T-shaped structure can be obtained by bringing in the Ar through either the "b" or "c" axis of the dimer. The plane of symmetry in the dimer is "ac" plane. With reference to Fig. 1, Ar approaching from above and below through "c" axis, leads to different values of rotational constants. However, for approach through "b" axis, both directions (from behind or front) are symmetric. Intuitively, one would expect the approach through the "b" axis. In fact, Dykstra's MMC calculations predict the global minimum with Ar on the "b" axis of the dimer.[15] In order to experimentally verify this, rotational constants for the various isotopomers were calculated for the three different possibilities using rigid structures.

Starting from the $(H_2O)_2$ geometry,[23] it was found that if Ar is kept on the dimer "c" axis, either above or below, the A rotational constant of trimer automatically increased compared to $(B+C)/2$ for the dimer, as found in the experiment. However, if Ar is kept on the dimer "b" axis, the R_{O-O} had to be reduced by 0.038 Å in order to reproduce the experimental A. A rigid structure could not fit A, B, and C of the trimer, simultaneously. For all three structures, a best possible fit of the three rotational constants was obtained. With these structures, the rotational constants for the three $(H_2\,{}^{18}O)$ containing trimers were calculated. It was noted that the change in the A rotational constant between Ar–$(H_2O-H_2\,{}^{18}O)$ and Ar–$(H_2\,{}^{18}O-H_2O)$ was very different for the three structures. For Ar in the dimer "c" axis above and below, this difference was 90 and −11 MHz, respectively. For Ar in the dimer "b" axis, it was 35 MHz. The experimental value is 36.6 MHz, clearly supporting the structure in which Ar is placed on the "b" axis of the dimer. It appears that the reduction in O–O distance by 0.035 Å on going from $(H_2O)_2$ to Ar–$(H_2O)_2$ is real. It is one order of magnitude larger than the 0.003 Å *increase* seen for the c.m.–c.m. distance between C_6H_6 and H_2O in $C_6H_6-H_2O$ dimer on addition of Ar to form the Ar–$C_6H_6-H_2O$ trimer.[20,25]

B. Rotational-tunneling energy levels

As indicated earlier, the "a" dipole transition from the A_1 state appeared at either higher or lower frequency compared to the transition from E state for Ar–$(H_2O)_2$. It should be pointed out now that the two tunneling motions considered earlier should give identical frequencies for "a" dipole transition from the three states, A_1, B_1, and E_1. The fact that they give frequencies differing by a few 100 kHz shows evidence for smaller perturbations not considered here. Independent fitting of the transitions from A_1 state leads to an rms deviation of about 456 kHz for Ar–$(H_2O)_2$ but only 3 kHz for Ar–$(D_2O)_2$. Clearly, the perturbation is more important for the fully protonated trimer and its effect is negligible for the deuterated species. Having stated this, we examine the ordering of the three states for some of the lower rotational levels. Only the interconversion splitting is considered and the much larger splitting due to the 180° rotation of the acceptor unit is neglected. Our experiments cannot determine this splitting.

Figure 2 shows the energy level diagrams for 0_{00} to 2_{11}

states of the trimer. The ordering of the A_1, E_1, and B_1 levels should be the same for levels connected by ''a'' dipole allowed transitions which showed a rigid rotor type spectra for all three states. It should be reversed for the ''b'' dipole allowed transitions. Only $K_p=0$ and 1 levels are shown and they are stacked separately to identify the ''a'' dipole and ''b'' dipole transitions. The ''a'' dipole transitions occur within the same K_p manifold and the ''b'' dipole transitions occur across the two manifolds. From the diagram, it is immediately obvious that for the ''b'' dipole transitions with K_p'' even, the transition frequencies increase in the order $A_1>E_1>B_1$. For the ''b'' dipole transitions with K_p'' odd this order is reversed with $A_1<E_1<B_1$.

The above analysis clearly points out the following: For $Ar-(D_2O)_2$, the ''b'' dipole transitions that were observed at lower and higher frequencies compared to the transitions from the E_1 state, should have contributions from both A_1 and B_1 states. The K_p'' for the transition determines where the A_1 and B_1 transitions are with respect to E_1 transition. In our spectral fitting discussed in the previous section for $Ar-(D_2O)_2$, this situation was not obvious. The lower transitions and upper transitions were fit independently as though they arise from the same states (Table II). This observation reinforces the point noted in the above-mentioned. For the fully deuterated trimer, the perturbation(s) from other tunneling motions not considered here are negligible.

C. Barrier to interchange tunneling

For the $(H_2O)_2$ and $(D_2O)_2$, Karyakin *et al.* modeled the interchange tunneling as resulting from a geared internal rotation of the two water units about their C_2 axis.[26] They used the following Hamiltonian to calculate the energy levels:

$$H=Fp^2+V_4/2(1-\cos 4\alpha). \tag{5}$$

They used F as $b_0/2$ where b_0 is the zero-point rotational constant of H_2O/D_2O about its ''b'' axis. The Hamiltonian matrix was set up in the free rotor basis $|m\rangle=e^{im\alpha}/(2\pi)^{1/2}$ and diagonalized to obtain eigenvalues. The tunneling splittings observed for the $(H_2O)_2$ and $(D_2O)_2$ were 22 554.37 and 1172.11 MHz and from these V_4 was calculated as 437 and 402 cm^{-1} for the two dimers, respectively.[21,26]

If one assumes that the interchange tunneling in the trimer does not involve motion of Ar, similar analysis can be done to estimate the barrier for this motion. Such an analysis for $Ar-(D_2O)_2$ with the tunneling splitting of 106.3 MHz, gives $V_4=642\ cm^{-1}$. It suggests that the barrier to donor-acceptor interchange tunneling in $(D_2O)_2$ increases from 402 to 642 cm^{-1} due to the formation of the trimer. If the barrier for $Ar-(H_2O)_2$ is increased by comparison, it shows that the splitting in the trimer could be of the order of 4–5 GHz. The A_1 transition is expected either at a higher or lower frequency than the E_1 transition, depending on K_p''. Hence, finding the ''b'' dipole rotational tunneling spectra from the A_1 state for $Ar-(H_2O)_2$ appears to be a difficult task with our spectrometer.

V. CONCLUSIONS

Rotational-tunneling spectra have been observed for $Ar-(H_2O)_2$, $Ar-(D_2O)_2$, $Ar-(H_2{}^{18}O)_2$, $Ar-(H_2{}^{16}O-H_2{}^{18}O)$ and $Ar-(H_2{}^{18}O-H_2{}^{16}O)$ trimers using a Balle–Flygare FTMW spectrometer. The observed tunneling levels could be correlated to the tunneling levels of the free water dimer. From the E^+ state rotational constants of the parent and $H_2{}^{18}O$ containing isotopomers, R_{O-O} distance has been estimated as 2.945 Å. This is 0.035 Å shorter than R_{O-O} in the water dimer. The trimer is T-shaped and the rotational constants for the H_2O and $H_2{}^{18}O$ containing isotopomers were used to infer that the Ar atom approaches through the ''b'' axis of the water dimer, rather than the ''c'' axis. An approximate analysis gives Ar-c.m.(H_2O) distance to be 3.637 Å, which is almost identical to that of $Ar-H_2O$ dimer.

The ''a'' dipole transitions from A_1 and E_1 states of $Ar-(H_2O)_2$ trimer were observed while the ''b'' dipole transitions were observed only for the E_1 state. Spin statistical weight for the B_1 state of $(H_2O)_2$ is 0, and hence, could not be observed. For $Ar-(D_2O)_2$, both ''a'' and ''b'' dipole transitions from all the three states could be observed. The ''b'' dipole transitions are split due to the donor–acceptor interchange tunneling. The tunneling splitting is determined to be 106.3 MHz for $Ar-(D_2O)_2$ compared to 1172 MHz for the $(D_2O)_2$. Assuming that the interchange tunneling does not involve motion of Ar, the barrier for this motion is estimated to be 642 cm^{-1}. As expected, the $Ar-(H_2{}^{16}O-H_2{}^{18}O)$ trimer did not show any doubling of the ''a'' dipole transitions due to the donor–acceptor interchange tunneling, since it leads to a different trimer. However, the $Ar-(H_2{}^{18}O-H_2{}^{16}O)$ trimer showed some doubling in *both* ''a'' and ''b'' dipole transitions due to some perturbation that has not been addressed.

ACKNOWLEDGMENTS

This report is based upon work supported by the Physical Chemistry Division of the National Science Foundation under Grant Nos. CHE 94-13380 and CHE 94-03545. The authors thank C. E. Dykstra for communicating some of his unpublished results and also for comments on an earlier version of the manuscript. Also thanked is G. T. Fraser for stimulating discussions and for educating the authors on the complexities of the water dimer system. He also provided the Fortran code, NFOLD.FOR, for calculating the torsional energy levels. The author E.A. thanks the Department of Science and Technology, India and the Director of the Indian Institute of Science for partial travel support, which facilitated completion of this manuscript.

[1] R. C. Cohen, K. L. Busarow, K. B. Laughlin, G. A. Blake, H. Havenith, Y. T. Lee, and R. J. Saykally, J. Chem. Phys. **89**, 4494 (1988).
[2] G. T. Fraser, F. J. Lovas, R. D. Suenram, and K. Matsumura, J. Mol. Spectrosc. **144**, 97 (1990).
[3] S. Suzuki, R. E. Bumgarner, P. A. Stockman, P. G. Green, and G. A. Blake, J. Chem. Phys. **94**, 824 (1991).
[4] R. Lascola and D. J. Nesbitt, J. Chem. Phys. **95**, 7917 (1991).
[5] T. Germann and H. S. Gutowsky, J. Chem. Phys. **98**, 5235 (1993).

[6] J. M. Hutson, J. Chem. Phys. **92**, 157 (1990).
[7] G. Chalasinski, M. M. Szcesniak, and S. Scheiner, J. Chem. Phys. **94**, 2807 (1991).
[8] M. Bulski, P. E. S. Wormer, and A. van der Avoird, J. Chem. Phys. **94**, 8096 (1991).
[9] C. Bissonnette and D. C. Clary, J. Chem. Phys. **97**, 8111 (1992).
[10] R. C. Cohen and R. J. Saykally, J. Chem. Phys. **98**, 6007 (1993), and papers cited therein.
[11] E. Arunan, T. Emilsson, and H. S. Gutowsky, J. Am. Chem. Soc. **116**, 8418 (1994).
[12] E. Arunan, C. E. Dykstra, T. Emilsson, and H. S. Gutowsky, J. Chem. Phys. **105**, 8495 (1996).
[13] E. Arunan, T. Emilsson, H. S. Gutowsky, and C. E. Dykstra, J. Chem. Phys. **114**, 1242 (2001).
[14] C. E. Dykstra, J. Am. Chem. Soc. **111**, 6168 (1989).
[15] C. E. Dykstra (personal communication).
[16] For a review see: G. T. Fraser, Int. Rev. Phys. Chem. **10**, 189 (1991).
[17] T. R. Dyke, J. Chem. Phys. **66**, 492 (1977).
[18] E. N. Karyakin, G. T. Fraser, and R. D. Suenram, Mol. Phys. **78**, 1179 (1993).
[19] T. J. Balle and W. H. Flygare, Rev. Sci. Instrum. **52**, 33 (1981); C. Chuang, C. Hawley, T. Emilsson, and H. S. Gutowsky, *ibid.* **61**, 1629 (1990).
[20] H. S. Gutowsky, T. Emilsson, and E. Arunan, J. Chem. Phys. **99**, 4883 (1993).
[21] E. N. Karyakin, G. T. Fraser, F. J. Lovas, R. D. Suenram, and M. Fujitake, J. Chem. Phys. **102**, 1114 (1995).
[22] T. A. Hu and T. R. Dyke, J. Chem. Phys. **91**, 7348 (1989).
[23] T. R. Dyke, K. M. Mack, and J. S. Muenter, J. Chem. Phys. **66**, 498 (1977).
[24] W. Gordy and R. L. Cook, *Microwave Molecular Spectra* (Wiley, New York, 1984), Chap. XIII.
[25] E. Arunan, T. Emilsson, and H. S. Gutowsky, J. Chem. Phys. **101**, 861 (1994).
[26] E. N. Karyakin, G. T. Fraser, and R. D. Suenram, Mol. Phys. **78**, 1179 (1993).